Published in final edited form as:
Angew Chem Int Ed Engl. 2013 April 8; 52(15): 4169–4173. doi:10.1002/anie.201210359.

A Plasmon-Assisted Optofluidic System for Measuring the Photothermal Conversion Efficiencies of Gold Nanostructures and Controlling an Electrical Switch

Jie Zeng[‡], **David Goldfeld**, and **Younan Xia**[†]
Department of Biomedical Engineering, Washington University in St. Louis, Saint Louis, Missouri 63130 (USA)

Abstract

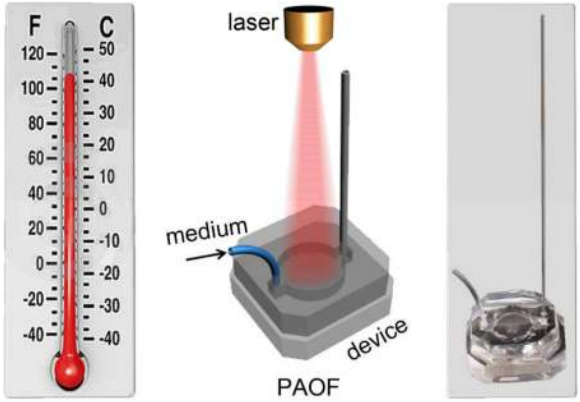

An optofluidic system was constructed from a diode laser as the energy source, an aqueous suspension of plasmonic nanostructures as the photothermal transducer, and a glass capillary for measuring the volumetric expansion of the suspension. The suspension could be driven to move up the capillary by more than 30 mm and be used to control the operation of an electrical switch.

Keywords

optofluidics; plasmonic nanostructures; photothermal conversion; absorption cross section

In localized surface plasmon resonance (LSPR), the conduction electrons of a plasmonic nanostructure are driven by the alternating electric field of an incident light to collectively oscillate at a resonant frequency.[1,2] As a result, the incident light will be absorbed by the plasmonic nanostructure. Some of the absorbed energy will be emitted as light through scattering while the rest will be dissipated by Landau damping,[3] resulting in light-to-heat conversion. The photothermal conversion has been used to induce localized heating of the

Correspondence to: Younan Xia.
[†]Current address:
The Wallace H. Coulter Department of Biomedical Engineering, Georgia Institute of Technology and Emory University, Atlanta, Georgia 30332 (USA), School of Chemistry and Biochemistry, School of Chemical and Biomolecular Engineering, Georgia Institute of Technology, Atlanta, Georgia 30332 (USA), younan.xia@bme.gatech.edu
[‡]Hefei National Laboratory for Physical Sciences at the Microscale and Department of Chemical Physics, University of Science and Technology of China, Hefei 230026, Anhui, P. R. China

Supporting information for this article is available on the WWW under http://dx.doi.org/.

host medium,[4] which is of great interest for applications in a number of fields, including photonics,[5] electronics,[6] catalysis,[7] phase transformation,[8] and biomedicine.[9]

The photothermal heating based on plasmonic nanostructures has also be been explored to induce and/or control fluid motion.[10] In the first demonstration, Lee and co-workers were able to drive liquid to move along microfluidic channels over a distance as far as 500 μm by using plasmonic heating with Au colloids.[11] In this case, the liquid was driven to move through a complex mechanism that involved a combination of localized evaporation, condensation, and surface wetting. In another demonstration, Wu and co-workers were able to control liquid flow through microfluidic channels by combining the temperature-dependent sol-gel transformation with a composite of Au nanorod and poly(dimethyl siloxane) to generate localized obstructions within specific paths.[12] Most recently, Halas and co-workers exploited the localized heating of SiO_2/Au nanoshells within a solution to vaporize water and ethanol with sunlight.[13] The nanoshells were thought to heat up rapidly upon irradiation and their surfaces were surrounded by thin layers of high-temperature vapor that carried the nanoshells to the top of the suspension before the vapor was released into the atmosphere above.

Despite these reported demonstrations, we noticed that the absorption cross sections of the plasmonic nanostructures, a fundamental property that determines their photothermal conversion efficiencies, were seldom measured experimentally in these studies. A quantitative understanding of this parameter is essential to the engineering of plasmonic nanostructures for a variety of applications like fluid transport, optical imaging contrast enhancement, and cancer treatment. In a prior study, we demonstrated the use of photoacoustic imaging for experimental measurements of the absorption cross sections of Au nanostructures, but this approach requires expensive equipment and complex procedures.[14]

Herein, we report a plasmon-assisted optofluidic (PAOF) system that is consisted of a diode laser as the energy source, an aqueous suspension of Au nanostructures as the photo-responsive fluidic medium, and a capillary as the means to monitor the change in temperature caused by volumetric expansion of the medium. Three different types of Au nanostructures were compared in this study: nanocages, nanorods, and hexapods; all of them can be tuned to absorb light in the near-infrared region. To achieve controllable fluid motion, we took advantage of the well-known thermal expansion phenomena of a liquid. With this system, we could drive a fluid to rise in a capillary by as much as 30 mm, depending on the type of nanostructures suspended in the medium and/or the concentration. We could also experimentally measure the absorption cross sections and photothermal conversion efficiencies of various types of plasmonic nanostructures. Furthermore, we demonstrated the feasibility of utilizing the fluid motion caused by plasmonic heating to construct a photo-sensitive electrical switch.

Figure 1a shows a schematic of the PAOF system. It contained a diode laser with a central output wavelength at 808 nm, a photo-responsive medium, and a microfluidic device illustrated in Figure 1b. The microfluidic device was assembled from a poly(dimethyl siloxane) (PDMS) block (***1***) with flat surface, a PDMS block patterned with a reservoir (***2***) on the surface, a plastic tube with an inner diameter of 0.5 mm (***3***) that serves as a channel for pumping in the liquid medium, and a glass capillary with an inner diameter of 0.6 mm (***4***) serving as a “ruler” to measure volumetric expansion of the liquid. All joints were sealed with PDMS. The exact dimensions of these components are summarized in Figure S1. In a typical experiment, 0.7 mL of a medium containing the plasmonic nanostructures was loaded, through the plastic tube, into the reservoir between blocks ***1*** and ***2*** until the medium reached a height of 1 cm in the capillary. The opening on tube ***3*** was then plugged with a

short glass rod. Since PDMS is transparent in the visible and near-infrared regions, the diode laser was able to penetrate through the top PDMS block to reach the liquid medium containing the plasmonic nanostructures. As such, the medium was quickly heated to a temperature as high as *ca.* 84 °C, depending on the type of nanostructures contained in the medium and their concentration. The medium then thermally expanded into capillary ***4*** due to the increase in temperature and the height of the liquid column was recorded during irradiation with a stationary camera. Figure 1C shows a photograph of the actual microfluidic device.

In the initial study, we compared the performance of three different types of Au plasmonic nanostructures: nanocages, nanorods, and hexapods. All of them can be engineered to generate heat through absorption of near-infrared light. The detailed procedures for the syntheses of these nanostructures can be found in the Supporting Information. Figure 2, a–c, shows transmission electron microscopy (TEM) images of these nanostructures. The nanocages in Figure 2a exhibited a porous morphology (with a hollow interior and pores at the corner sites) with an edge length of 45 nm and a wall thickness of *ca.* 5 nm.[15] The nanorods in Figure 2b had an average diameter of 17 nm and an aspect ratio of *ca.* 3.3.[16] The hexapods in Figure 2c showed a highly branched morphology with an octahedral core of *ca.* 25 nm in edge length and six arms on all the vertices.[17] The distance between the ends of two opposite vertices was *ca.* 60 nm. In principle, the LSPR peaks of all these nanostructures can be precisely tuned to any wavelength in the near-infrared region by adjusting their wall thickness, aspect ratio, and arm length, respectively. In this study, all of their major LSPR peaks were tuned to the region of 805–810 nm to match the central output wavelength (808 nm) of the diode laser. Figure 2d shows UV-vis-NIR extinction spectra of these three different types of Au nanostructures.

We used an organic dye, indocyanine green (ICG), as a reference of calibration. To establish a relationship between the temperature and the height of liquid in the capillary, we calibrated the PAOF system by adding 0.7 mL of 6.5 μM ICG solution into the device, irradiating the medium with the diode laser, monitoring the temperature (T) of the medium in real time with an infrared camera, and recording the height (h) of the medium in capillary ***4*** whenever the temperature reached the specific values of 24, 37, 50, and 70 °C. The power density of the laser was set to 0.4 $W \cdot cm^{-2}$ and the illumination area was 1.13 cm^2 for all the experiments. As shown in Figure S2, a linear relationship was found between h and T. The slope ($\Delta h/\Delta T$) was calculated to be 0.52 mm $°C^{-1}$. Since all the media we used were based on aqueous solutions and they should have more or less the same volumetric expansion coefficient, it is not unreasonable to assume that the calibration value for $\Delta h/\Delta T$ can also be applied to media containing different types of Au nanostructures. The linear relationship between h and T suggests that one can determine the temperature of a medium by simply measuring the height (h) of liquid in the capillary, just like a thermometer.

We then evaluated the plasmon-assisted heating process over a period of 40 min: the diode laser was turned on for 10 min to heat the medium, and then turned off for 30 min to let the medium cool down. This process was repeated three times and the height was recorded at an interval of one minute. For nanocages, we made measurements for four different concentrations at 1.0×10^9, 2.5×10^9, 5.0×10^9, and 1.0×10^{10} particles/mL (Figure 3a) while we only examined one concentration of 1.0×10^{10} particles/mL for both nanorods and hexapods (Figure S3). The curves clearly show the periodicity of change in height (Δh). As expected, the Δh value increased with the concentration of the nanostructures due to the increased power of absorption for the solution. For nanocages of 1.0×10^{10} particles/mL in concentration, we were able to drive the fluid up to a height of *ca.* 30.5 mm in the capillary. We then calculated the change in temperature (ΔT) based on the calibration value for $\Delta h/\Delta T$ and the results are summarized in Table 1. For nanocages with different concentrations,

the ΔT varied from *ca.* 11.2 to *ca.* 58.7 °C, which corresponded to a maximum temperature of 82.7 °C when we started from room temperature (24 °C). For nanorods and hexapods, the ΔT values were less than half of that for nanocages at the same particle concentration.

To quantitatively evaluate the capability of converting light into heat for different types of plasmonic nanostructures, we calculated the energy conversion efficiency (η) using the following equation:

$$\eta = Q/E \quad (1)$$

where Q is the total heat generated in the solution which depends on ΔT for a given particle concentration and E is the total energy output of the laser over the 10-min period (both of them are defined and derived in the Supporting Information). Table 1 summarizes Δh, ΔT, and η for nanocages, nanorods, and hexapods at various concentrations. As the concentration of nanocages increased from 1.0×10^9 to 2.5×10^9, 5.0×10^9, and 1.0×10^{10} particles/mL, η increased from 12.1±0.8% to 27.9±1.7%, 46.9±2.9%, and 63.6±4.2%, respectively (see Table 1 and Figure 3b). For nanorods and hexapods at a concentration of 1.0×10^{10} particles/mL, their η values were 22.1±1.7% and 29.6±1.9%, respectively, which were less than half of that for nanocages at the same concentration. The disparity in η for the three types of nanostructures is believed to be caused by their differences in absorption coefficient (μ) associated with absorption cross section (σ), an intrinsic property of the plasmonic nanostructure that determines its ability to absorb light at a particular wavelength.

One of the major applications of the PAOF system is to experimentally measure the μ and thus calculate the σ of a plasmonic nanostructure. To demonstrate this capability, we used ICG as a reference again because its absorption coefficient (μ_{ICG}, which equals to 140 m^{-1}) is well documented.[18] After adding 0.7 mL of 6.5 μM ICG solution into the device, we irradiated the system for 10 min and a change in height (Δh_{ICG}) of 33.2 mm was measured. We then derived the μ associated with the σ of a plasmonic nanostructure by firstly calculating the heat (Q) from eq. (S1). The irradiation energy being absorbed (E_{abs}) can be expressed as eq. (S4). Since the absorbed energy (E_{abs}) is completely converted to heat (Q) through Landau damping,[3] we obtain eq. (S6). When the same device is used for both ICG and a suspension of Au nanostructures, the following equation can be used to calculate the μ of the nanostructure (μ_{NS}):

$$\mu_{NS} = -\frac{1}{x}\ln\left[1 - \frac{\Delta h_{NS}}{\Delta h_{ICG}}\left(1 - e^{-\mu_{ICG}x}\right)\right] \quad (2)$$

After obtaining μ_{NS} from eq. (2) at the particle concentrations shown in Table 1, we calculated σ using the following equation.[14,19]

$$\sigma = \frac{\mu}{MN_A} \quad (3)$$

where M is the molar concentration of the nanostructures and N_A is the Avogadro's constant.

The experimentally obtained μ and σ are listed in Table 1 for each type of Au nanostructure at different concentrations. The magnitude of σ for the nanocages was on the same order as what was derived from theoretical calculations (16.3×10^{-15} m^2),[14] suggesting that the PAOF system can be adopted for quantitative measurements of μ and σ. When comparing the σ values of the three different types of Au nanostructures, we found that the nanocages had the highest magnitude while the nanorods had the lowest and the values of σ for both nanorods and hexapods were less than half of that of nanocages. This finding agrees with the

observed trend for η, in which nanocages exhibited the highest efficiency in converting light to heat. Although prior studies demonstrated that the σ of plasmonic nanostructures could be measured by either photoacoustic imaging[14] or optical coherence tomography,[20] the technique reported in this study provides a much simpler and more convenient tool as it does not require any specific equipment or training.

By taking advantage of the light-driven motion of liquid in a PAOF system, we demonstrated a photo-sensitive electrical switch. In this case, we saturated an aqueous suspension of Au nanocages (1.0×10^{10} particles/mL) with NaCl to make it conductive and then used as the fluidic medium. As shown in Figures 4a and S4, we constructed the switch from a small vial connected to a capillary containing two standard copper wires with a gap of 5 mm between their ends (as marked by * and ** symbols in Figure 4a). When the solution was irradiated by the diode laser, it heated up and expanded along the capillary, bridging the gap between the two wires and completing an electrical circuit. The connection turned on a small light-emitting diode (LED). After turning off the laser irradiation, the solution level dropped and the LED was switched off. As shown in Figure 4b, the electrical switch could be operated through four cycles of on and off irradiations without losing its performance, suggesting that it could be used to control electrical devices without requiring mechanical movement or large solid-state transistors. To our knowledge, this was the first example demonstrating the potential use of fluid motion controlled by plasmonic heating to construct a functional electrical device.

In summary, we have demonstrated a plasmon-assisted optofluidic system by combining the unique features of microfluidics and plasmonic heating of noble-metal nanostructures. By taking advantage of the well-known thermal expansion of a liquid, we could move a fluid column via plasmonic heating. Using this simple system, we were able to quantitatively measure the photothermal conversion efficiencies of various plasmonic nanostructures and their absorption cross sections. We also demonstrated the feasibility of constructing a photo-sensitive, electrical switch by controlling the liquid level with plasmonic heating. Our plasmon-assisted optofluidic system provides a simple and effective platform for remotely controlling the motion of a fluid and is expected to find use in various areas involving molecular transport, biochemical analysis, catalysis, photonics, and electronics.

Supplementary Material

Refer to Web version on PubMed Central for supplementary material.

Acknowledgments

This work was supported in part by a research grant from NCI (1R01 CA138527), an NIH Director's Pioneer Award (DP1, OD00798), and startup funds from Washington University in St. Louis and Georgia Institute of Technology. Y.X. was also partially supported by the World Class University (WCU) program through the National Research Foundation of Korea funded by the Ministry of Education, Science and Technology (R32-20031).

References

1. a) Govorov AO, Richardson HH. Nano Today. 2007; 2:30.b) Hirsch LR, Stafford RJ, Bankson JA, Sershen SR, Rivera B, Price RE, Hazle JD, Halas NJ, West JL. Proc. Natl. Acad. Sci. U.S.A. 2003; 100:13549. [PubMed: 14597719] c) Rycenga M, Cobley CM, Zeng J, Li W, Moran CH, Zhang Q, Qin D, Xia Y. Chem. Rev. 2011; 111:3669. [PubMed: 21395318] d) Hu M, Wang X, Hartland GV, Mulvaney P, Juste JP, Sader JE. J. Am. Chem. Soc. 2003; 125:14925. [PubMed: 14640670]
2. a) Link S, El-Sayed MA. Annu. Rev. Phy. Chem. 2003; 54:331.b) Barnes WL, Dereux A, Ebbesen TW. Nature. 2003; 424:824. [PubMed: 12917696] c) Kelly KL, Coronado E, Zhao LL, Schatz GC. J. Phys. Chem. B. 2003; 107:668.d) Willets KA, Van Duyne RP. Annu. Rev. Phys. Chem. 2007; 58:267.. [PubMed: 17067281]

3. Gao Y, Yuan Z, Gao S. J. Chem. Phys. 2011; 134:134702. [PubMed: 21476764]
4. a) Lukianova-Hleb E, Hu Y, Latterini L, Tarpani L, Lee S, Drezek RA, Hafner JH, Lapotko DO. ACS Nano. 2010; 4:2109. [PubMed: 20307085] b) Jain PK, El-Sayed IH, El-Sayed MA. Nano Today. 2007; 2:18.c) Carlson MT, Green AJ, Richardson HH. Nano Lett. 2012; 12:1534. [PubMed: 22313363] d) Ye EY, Win KY, Tan HR, Lin M, Teng CP, Mlayah A, Han MY. J. Am. Chem. Soc. 2011; 133:8506. [PubMed: 21563806] e) Ma HY, Bendix PM, Oddershede LB. Nano Lett. 2012; 12:3954. [PubMed: 22738210]
5. a) Schmidt H, Hawkins AR. Nat. Photonics. 2011; 5:598.b) Baffou G, Quidant R, García de Abajo FJ. ACS Nano. 2010; 4:709. [PubMed: 20055439] c) Ming T, Zhao L, Yang Z, Chen HJ, Sun LD, Wang JF, Yan CH. Nano Lett. 2009; 9:3896. [PubMed: 19754068]
6. a) Ozbay E. Science. 2006; 311:189. [PubMed: 16410515] b) Banerjee P, Conklin D, Nanayakkara S, Park T-H, Therien MJ, Bonnell DA. ACS Nano. 2010; 4:1019. [PubMed: 20095631]
7. a) Liu Z, Hou W, Pavaskar P, Aykol M, Cronin SB. Nano Lett. 2011; 11:1111. [PubMed: 21319840] b) Adleman JR, Boyd DA, Goodwin DG, Psaltis D. Nano Lett. 2009; 9:4417. [PubMed: 19908825] c) Christopher P, Xin H, Linic S. Nat. Chem. 2011; 3:41..
8. a) Ma H, Bendix PM, Oddershede LB. Nano Lett. 2012; 12:3954. [PubMed: 22738210] b) Moon GD, Choi S-W, Cai X, Li W, Cho EC, Jeong U, Wang LV, Xia Y. J. Am. Chem. Soc. 2011; 133:4762. [PubMed: 21401092] c) Zeng J, Roberts S, Xia Y. Chem. Eur. J. 2010; 16:12559.. [PubMed: 20945450]
9. a) Cobley CM, Chen J, Cho EC, Wang LV, Xia Y. Chem. Soc. Rev. 2011; 40:44. [PubMed: 20818451] b) Lal S, Clare SE, Halas NJ. Acc. Chem. Res. 2009; 41:1842. [PubMed: 19053240] c) Skirtach AG, Dejugnat C, Braun D, Susha AS, Rogach AL, Parak WJ, Mohwald H, Sukhorukov GB. Nano Lett. 2005; 5:1371. [PubMed: 16178241]
10. a) Erickson D, Sinton D, Psaltis D. Nat. Photonics. 2011; 5:583.b) Miao X, Wilson BK, Lin LY. Appl. Phys. Lett. 2008; 92:124108.c) Fan X, White IM. Nat. Photonics. 2011; 5:591. [PubMed: 22059090] d) Donner JS, Baffou G, McCloskey D, Quidant R. ACS Nano. 2011; 5:5457. [PubMed: 21657203]
11. Liu GL, Kim J, Lu Y, Lee LP. Nat. Mater. 2006; 5:27. [PubMed: 16362056]
12. Fang C, Shao L, Zhao Y, Wang J, Wu H. Adv. Mater. 2012; 24:94. [PubMed: 22144399]
13. Neumann O, Urban AS, Day J, Lal S, Nordlander P, Halas NJ. ACS Nano. 2013
14. Cho EC, Kim C, Zhou F, Cobley CM, Song KH, Chen J, Li Z-Y, Wang LV, Xia Y. J. Phys. Chem. C. 2009; 113:9023.
15. Zeng J, Zhang Q, Chen J, Xia Y. Nano Lett. 2010; 10:30. [PubMed: 19928909]
16. a) Nikoobakht B, El-Sayed MA. Chem. Mater. 2003; 15:1957.b) Sau TK, Murphy CJ. Langmuir. 2004; 20:6414. [PubMed: 15248731]
17. Kim D, Yu T, Cho E, Ma Y, Park O, Xia Y. Angew. Chem. Int. Ed. 2011; 50:6328.
18. Optical Absorption of ICG. http://omlc.ogi.edu/spectra/icg/index.html.
19. Wang, LV.; Wu, H. Biomedical Optics: Principles and Imaging. 1st ed.. New York: John Wiley and Sons; 2007.
20. Cang H, Sun T, Li Z-Y, Chen J, Wiley BJ, Xia Y, Li X. Opt. Lett. 2005; 30:3048. [PubMed: 16315717]

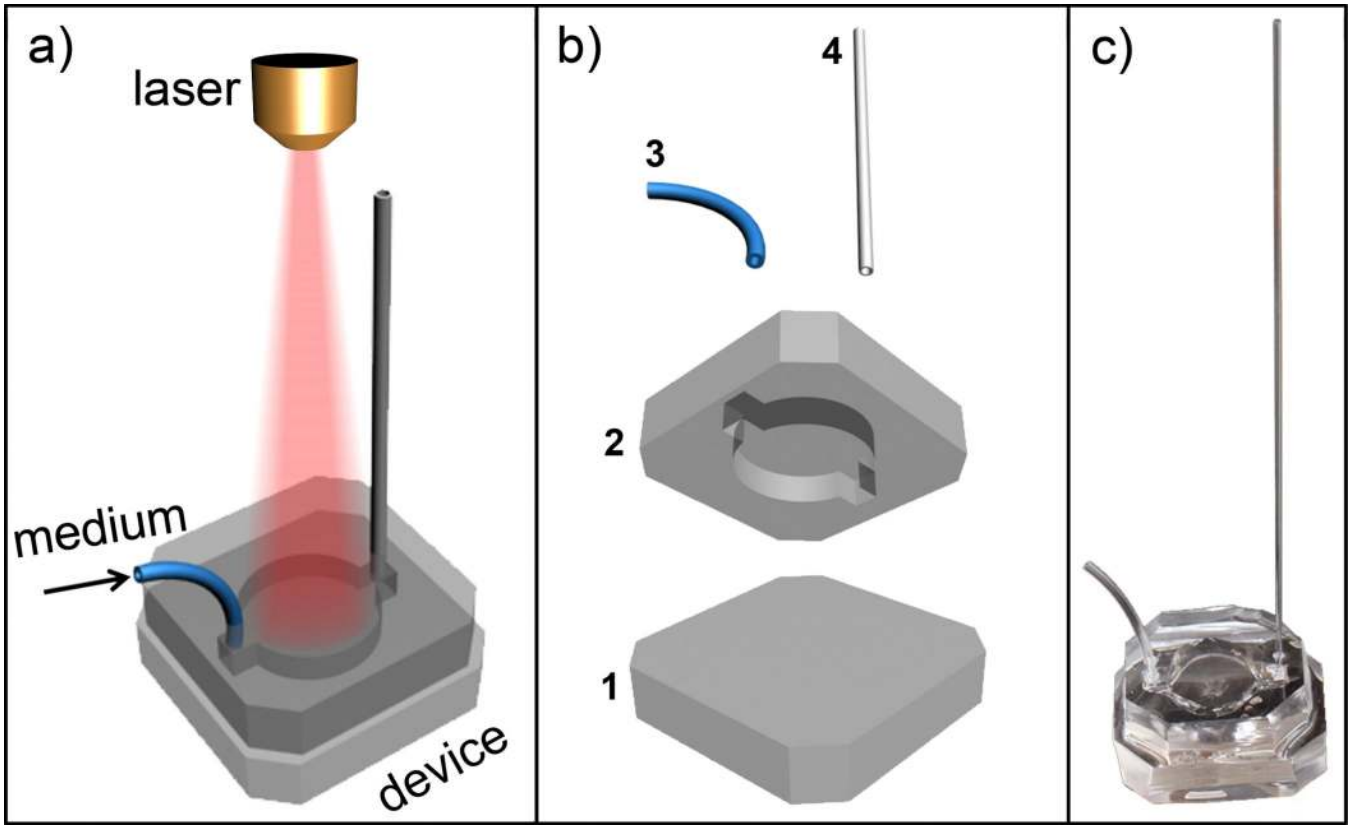

Figure 1.

a) A schematic of the plasmon-assisted optofluidic system. The arrow indicates the end of the plastic tube where the medium was pumped into the microfluidic device. b) A schematic drawing of the microfluidic device. ***1***: PDMS block used to seal the reservoir. ***2***: PDMS block cast with a reservoir to host the medium. ***3***: Plastic tube serving as a channel for pumping the medium. ***4***: Glass capillary used for measuring the volumetric expansion. c) Photograph of an assembled optofluidic system.

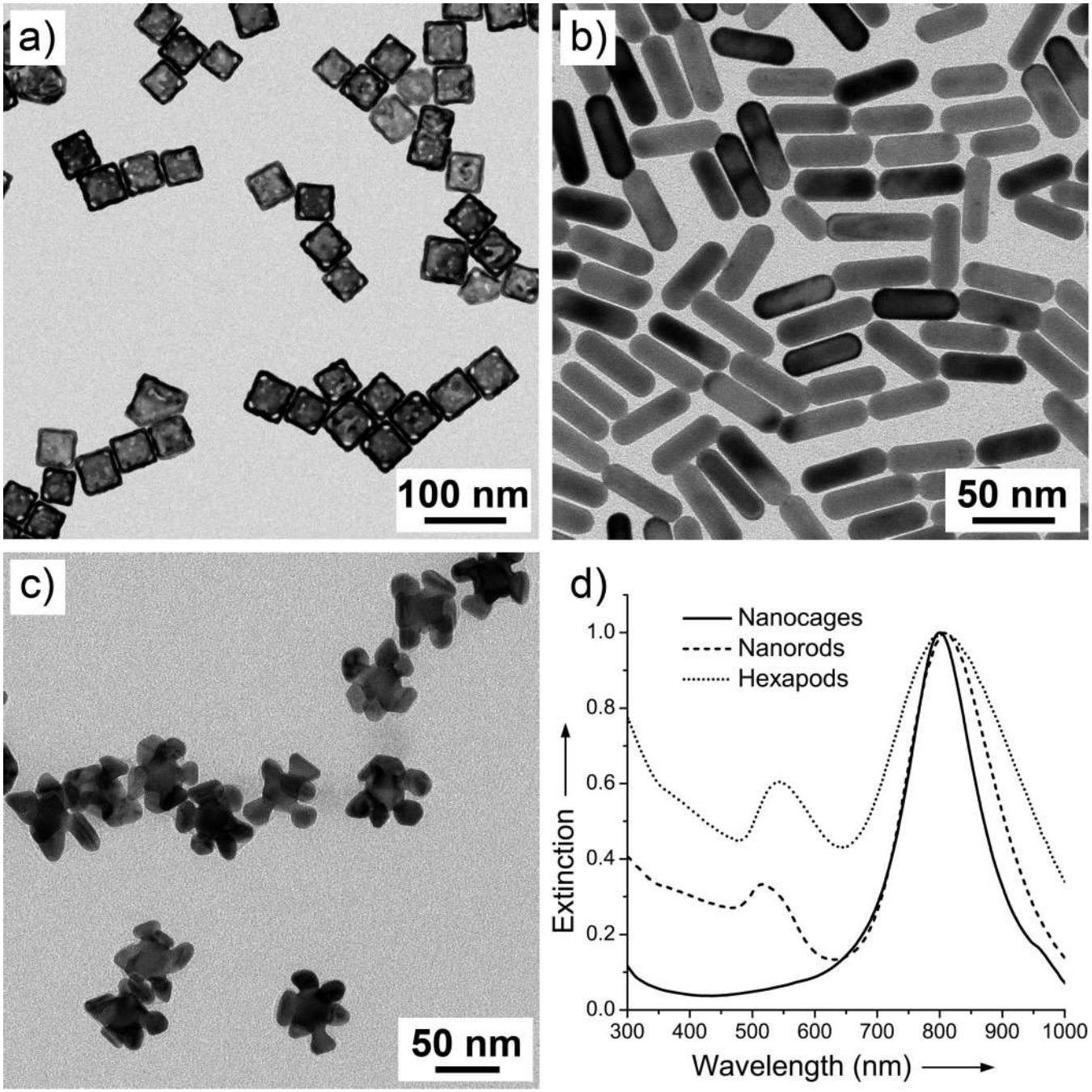

Figure 2.

TEM images of the three types of Au plasmonic nanostructures used for converting light into heat: a) nanocages with an outer edge length of 45 nm and a wall thickness of *ca.* 5 nm, b) nanorods with an average diameter of 17 nm and an aspect ratio of *ca.* 3.3, and c) hexapods with an average distance of *ca.* 60 nm between the ends of two opposite vertices. d) UV-vis-NIR extinction spectra of the three different types of Au nanostructures.

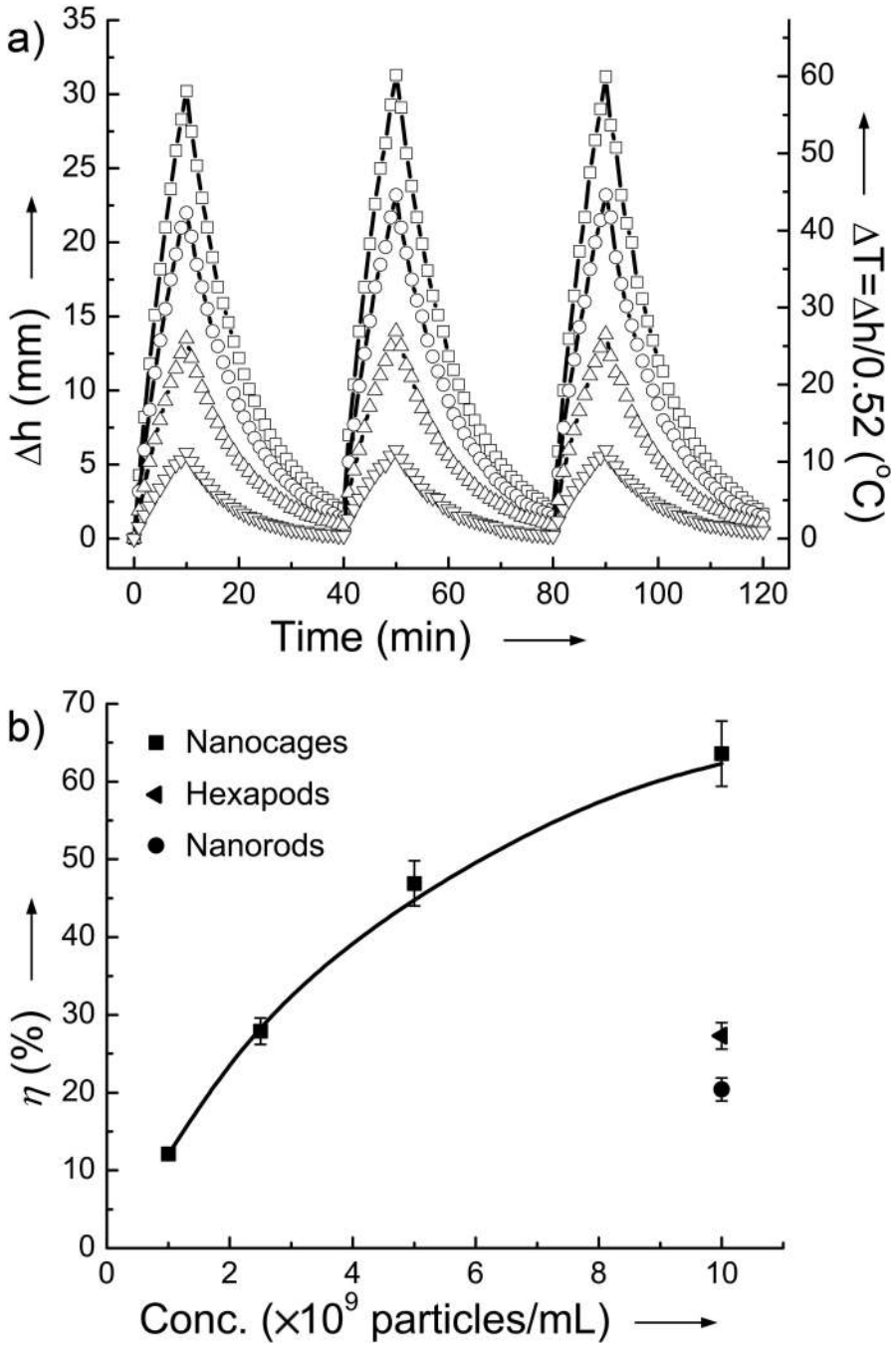

Figure 3.

a) Plot of the rise in height (Δh) and increase in temperature (ΔT) upon irradiation as a function of time when suspensions of Au nanocages of four different concentrations were used: 1.0×10^9, 2.5×10^9, 5.0×10^9, and 1.0×10^{10} particles/mL (from bottom to top). Each cycle of irradiation lasted for 40 min (on for 10 min and then off for 30 min) and the cycle was repeated three times. b) Plot of the energy conversion efficiency (η) as a function of particle concentration. For all the irradiation processes, the laser density was set to 0.4 W/cm^2 and the illuminated area was 1.13 cm^2.

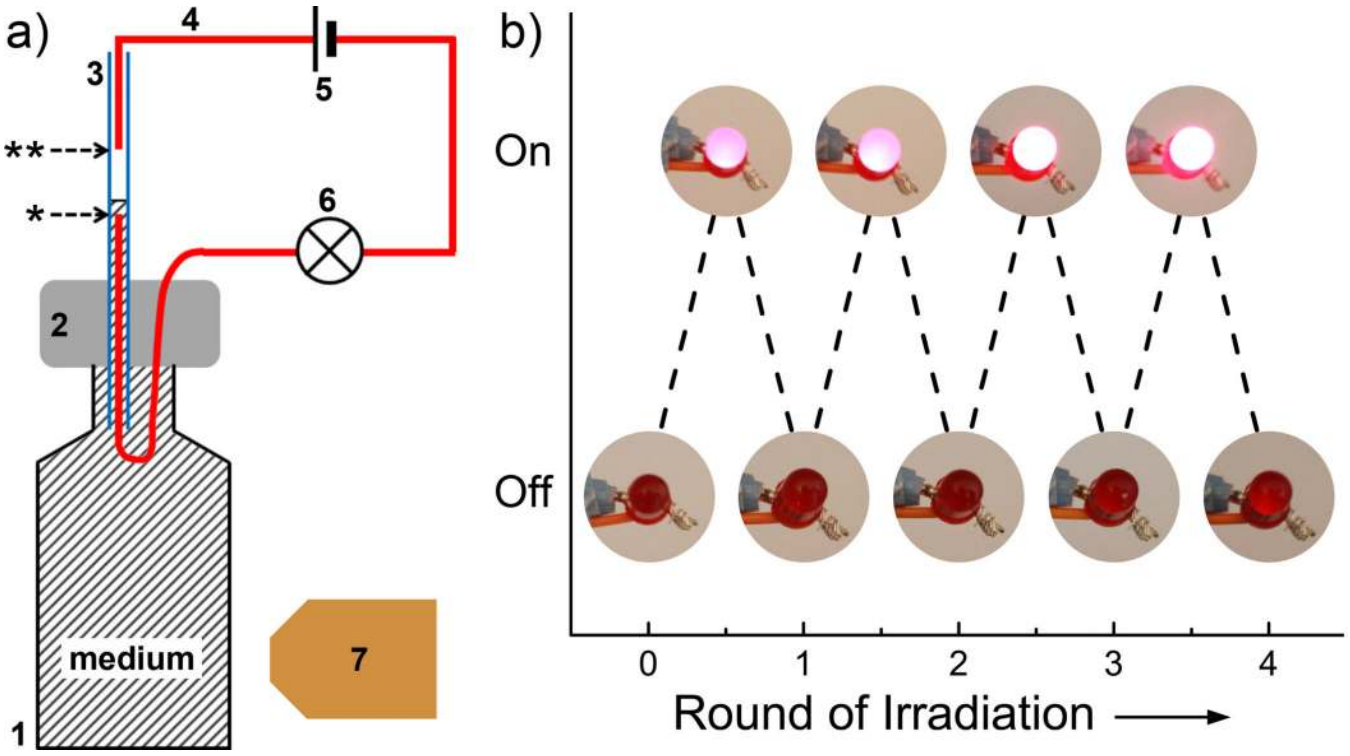

Figure 4.

a) Schematic illustration of a photo-responsive electrical switch. A 5-mL glass vial (***1***) was capped with a PDMS block (***2***) inserted with a 1.0-mm capillary tube (***3***). A standard copper wire (***4***) was used to connect the switch to three 1.5 V AA batteries (***5***) connected in series to a standard LED light bulb (***6***). A suspension of Au nanocages (1.0×10^{10} particles/mL) saturated with NaCl was loaded into the vial until it reached the top (*) of the lower copper wire but did not reach the bottom (**) of the upper wire. When the vial was irradiated with a diode laser (***7***), the solution expanded, filling tube ***3*** and bridging the 5-mm gap between the two copper wires, turning on the LED bulb. b) Demonstration of the on-off switching of a LED over four cycles.

Table 1

Comparisons of the rise in height (Δh), increase in temperature (ΔT), energy conversion efficiency (η), absorption coefficient (μ), and absorption cross section (σ) for Au nanocages, nanorods, and hexapods at different particle concentrations. For each measurement, the sample was irradiated for 10 min.

	Nanocages				Nanorods	Hexapods
Concentration (particles/mL)	**1.0×10^9**	**2.5×10^9**	**5.0×10^9**	**1.0×10^{10}**	**1.0×10^{10}**	**1.0×10^{10}**
Δh (mm)	5.8±0.4	13.4±0.8	22.5±1.4	30.5±2.0	10.6±0.8	14.2±0.9
ΔT (K)	11.2±0.8	25.8±1.5	43.3±2.7	58.7±3.8	20.4±1.5	27.3±1.7
η (%)	12.1±0.8	27.9±1.7	46.9±2.9	63.6±4.2	22.1±1.7	29.6±1.9
μ (m^{-1})	18.4±1.3	45.4±3.1	83.5±6.5	123.6±11.6	35.0±3.0	48.5±3.5
σ ($\times10^{-15}$ m^2)	18.4±1.3	18.2±1.2	16.7±1.3	12.4±1.2	3.5±0.3	4.9±0.4